ELSEVIER

Journal of Fluids and Structures 24 (2008) 295–312

JOURNAL OF FLUIDS AND STRUCTURES

www.elsevier.com/locate/jfs

Two-dimensional incompressible unsteady airfoil theory—An overview

D.A. Peters

Department of Mechanical, Aerospace and Structural Engineering, Washington University, Campus Box 1185, St. Louis, MO 63130, USA

Received 7 February 2007; accepted 2 September 2007
Available online 19 November 2007

Abstract

Two-dimensional unsteady airfoil theory has a history that dates back at least 75 years. Closed-form solutions have been obtained for airfoil loads due to step response (either to a pitch input or to a gust), due to airfoil oscillations in the frequency domain, and due to generalized airfoil motions in the Laplace domain. It has also been shown that the response of airloads to airfoil motions can be formulated in state space in terms of ordinary differential equations that approximate the airfoil and flow field response. The more recent of these models are hierarchical in that the states represent inflow shape functions that form a convergent series in a Ritz–Galerkin sense. A comparison of the various approaches with each other and with alternative computational approaches yields insight into both the methodologies and the solutions.

Keywords: Unsteady; Aerodynamics; Airfoil; Aeroelasticity

1. Introduction

1.1. Background

Two-dimensional unsteady airfoil theory (in particular for incompressible flow) has an interesting history that spans more than 75 years. The primary motivation of this work sprang from the practical interest in aeroelasticity and especially in fixed-wing flutter. Although two-dimensional incompressible potential flow theory is certainly a great simplification over the reality of airplane aerodynamics, it nevertheless gives reasonable answers to many questions of aeroelasticity, as well as keen insight into the aerodynamic mechanisms of unsteady airfoil behavior. Furthermore, the mathematics is tractable enough to allow powerful mathematical tools to contribute significantly to this insight.

1.2. Historical developments

Wagner (1925) published an expression for the indicial response of a two-dimensional, flat-plate airfoil in incompressible potential flow. Theodorsen (1934) presented the lift and pitching moment for this type of airfoil under

E-mail address: dap@me.wustl.edu

0889-9746/$ - see front matter
doi:10.1016/j.jfluidstructs.2007.09.001

Nomenclature

b	blade semi-chord, m
b_n	expansion coefficients
c	real part of s, constant for which all singularities are to the left of $c+ik$
$C(k)$	Theodorsen function
d	damping coupling matrix
$D(s)$	complex lift deficiency function
f_n, g_n	potential functions
$K_0(s)$	Bessel function of order zero
$K_1(s)$	Bessel function of order one
k	reduced frequency $\omega b/V$, Im$[s]$
L	lift, nondimensional
$L[\,]$	Laplace transform
L_b	lift due to total bound circulation
L_C	circulatory lift definition of Theodorsen (1934)
M	mass matrix
M_0	pitching moment about mid-chord, nondimensional
$M_{1/4}$	pitching moment about quarter chord, nondimensional
P_D	lift per unit length, nondimensional
p	pressure, N/m^2
Q	mass coupling matrix
S	damping matrix
s	Laplace transform variable in reduced time
t	reduced time V(time)$/b$
u,v	x and y velocity components, nondimensional on V
$\bar{u}(t)$	unit step function
v_b	part of v due to γ_b
v_w	part of v due to γ_w
V	free-stream velocity, m/s
w_n	components of total velocity field
$W(t)$	Wagner function
X	change of variable, $e^{-\eta}$
x,y	Cartesian coordinates nondimensional on b
β	eigenvalue
γ	vorticity per unit length
γ_b	bound vorticity
γ_w	wake vorticity
Γ	total bound circulation, nondimensional
$\hat{\Gamma}$	normalized circulation, $\Gamma/2\pi$
$\delta(t)$	impulse function
λ	downwash due to $\gamma_w = -v_w$
λ_n	coefficients of velocity due to shed wake
v	downwash due to bound vorticity, $= -v_b$
v_n	components of velocity due to bound vorticity
ξ	dummy variable of integration
ρ	density of air, kg/m^3
τ	nondimensional time in Peters and Karunamoorthy (1993, 1994), $\tau \equiv t$
τ_n	pressure expansion coefficients
ϕ,η	elliptical coordinates
Φ	nondimensional pressure, $p/\rho V^2$
Φ^A	acceleration potential
Φ_n	expansion functions for Φ
Φ^V	velocity gradient potential
Ψ	velocity potential
ω	frequency, rad/s
$(\,)_L$	lower surface, $\lim_{y\to 0^-} -1<x<+1$
$(\,)_U$	upper surface, $\lim_{y\to 0^+} -1<x<+1$
$\dot{(\,)}$	$\partial(\,)/\partial t$

simple harmonic motion. Part of this general solution is the theodorsen function, which is probably the best-known analytical expression that relates the effect of the shed wake on airfoil lift in the frequency domain. Garrick (1938) showed that the indicial response and Theodorsen function were related through a Fourier transform. R.T. Jones developed a two-state approximation to lift theory (Jones, 1938) which could be used in either the time domain (as an approximation to Wagner's indicial response), in the frequency domain (as an approximation to the Theodorsen function), in the differential equation domain (for time marching), or in the Laplace domain (for general airfoil motion) (Jones, 1939). Sears (1940) applied this operational form to some interesting problems of practical interest. W.P. Jones (1945) was the first to formulate an exact laplace domain version of the Theodorsen function. However, at that time there was concern as to whether or not this function was truly valid for negative real arguments of s (Edwards et al., 1989).

Later, renewed interest in two-dimensional aerodynamics centered around finite-state approximations to the Wagner, Theodorsen, and Laplace solutions. Hassig (1971) used rational functions in the Laplace domain to approximate the exact solutions. Vepa (1976) introduced the method of Padé approximants to give a finite-state representation of lift force in the frequency domain, as did Dowell (1980). Edwards et al. (1978, 1979) attacked both the incompressible and compressible airfoil behavior in two dimensions. They established the mathematical rigor of the Laplace domain generalization of the Theodorsen function, $D(s)$, and applied it numerically to problems of aeroelasticity.

It is interesting to note here that there is also a two-dimensional model of unsteady aerodynamics for rotary wings in which the returning wake is treated by layers of vorticity below the airfoil in a two-dimensional plane. Loewy (1957) used this concept to develop an analog to the Theodorsen function for rotary wings. Dinyavari and Friedmann (1984) used Padé approximants for the Loewy function to obtain finite-state models of rotary-wing aerodynamics. Other

rotary-wing researchers, in trying to accommodate the need for general motion theories in rotorcraft, have used the Wagner function in a convolution integral (Beddoes, 1983), thus ignoring the returning wake.

1.3. Other finite-state models

In addition to finite-state models developed as Padé fits to exact frequency response curves, other work has concentrated on the development of finite-state models from first principles. Peters and Karunamoorthy (1993, 1994) showed that a Glauert expansion of inflow states could be used to derive a set of ordinary differential state equations in which the states represented inflow distributions. The resultant equations give convergence to both Theodorsen and Wagner functions. Peters et al. (1995), also showed that a similar theory could be developed from an expansion of potential functions.

Peters and Johnson (1994) indicate that any of the two-dimensional theories (including the finite-state models) can be thought of as a feedback system in which inflow due to shed wake is an open-loop transfer function. The result is that a more easily applied theory can be utilized in which the inflow theory and airloads theory are modeled separately, so that closing the loop is done numerically in the assembled equations. They, along with Barwey, then utilized this concept to do correlations with several sets of experimental data (Peters et al., 1995).

1.4. Present work

In this paper, the theoretical bases of the various modeling approaches will be compared with some numerical results. These comparisons give insight into the nature of two-dimensional unsteady aerodynamics. These methods are also compared in principle to computational, finite-difference approaches to help to clarify the relationships among all approaches.

2. Basic equations

2.1. Fluid mechanics

The basic nondimensional equations from which all incompressible two-dimensional inflow models are obtained are continuity and momentum, as defined in the coordinates shown in Fig. 1, where lengths are nondimensional on semi-chord, velocities on free-stream, and pressure on ρV^2. Nondimensional (reduced) time follows, giving

$$\partial u/\partial x + \partial v/\partial y = 0, \tag{1}$$

$$\partial u/\partial t + \partial u/\partial x = -\partial \Phi/\partial x, \quad \partial v/\partial t + \partial v/\partial x = -\partial \Phi/\partial y \Phi. \tag{2}$$

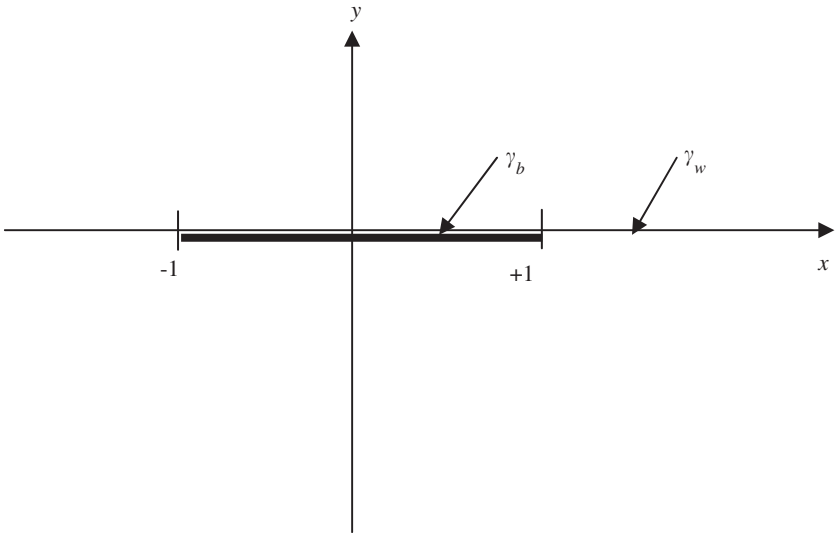

Fig. 1. Coordinate system.

These, along with the boundary conditions at the airfoil form thin-airfoil theory. Next, it is advantageous to form a velocity gradient potential Φ^V and an acceleration potential Φ^A.

$$\partial u/\partial x \equiv -\partial \Phi^V/\partial x, \quad \partial v/\partial x \equiv -\partial \Phi^V/\partial y, \quad \partial u/\partial t \equiv -\partial \Phi^A/\partial x, \quad \partial v/\partial t \equiv -\partial \Phi^A/\partial y. \tag{3}$$

It follows immediately from Eqs. (1) and (2) that

$$\partial^2 \Phi^A/\partial x^2 + \partial^2 \Phi^A/\partial y^2 = 0, \quad \partial^2 \Phi^V/\partial x^2 + \partial^2 \Phi^V/\partial y^2 = 0, \quad \Phi^A + \Phi^V \equiv \Phi. \tag{4}$$

Thus, the pressure Φ must also be a potential function.

2.2. Relationships between potentials

From the above derivation, one can derive relationships between the velocity fields and the potentials:

$$u = -\int_{-\infty}^{x} \frac{\Phi^V}{\partial x}\,\mathrm{d}x = -\Phi^V, \quad v = -\int_{-\infty}^{x} \frac{\partial \Phi^V}{\partial y}\,\mathrm{d}x, \tag{5}$$

$$\Phi^V = \int_{-\infty}^{t} \frac{\partial \Phi^A}{\partial x}\mathrm{d}t, \quad \Phi^A = \int_{-\infty}^{x} \frac{\partial \Phi^V}{\partial t}\,\mathrm{d}x, \tag{6}$$

$$\Phi = \Phi^A + \frac{\partial}{\partial x}\int_{-\infty}^{t} \Phi^A \mathrm{d}t, \quad \Phi = \Phi^V + \frac{\partial}{\partial t}\int_{-\infty}^{x} \Phi^V\,\mathrm{d}x, \tag{7}$$

$$\partial \Phi^A/\partial t + \partial \Phi^A/\partial x = \partial \Phi/\partial t, \quad \partial \Phi^V/\partial t + \partial \Phi^V/\partial x = \partial \Phi/\partial x. \tag{8}$$

The above relationships are useful in both the closed-form and the finite-state developments.

2.3. Vorticity and pressure

As a final piece of the mathematics, we define the nondimensional vorticity distribution, γ, and the lift per unit length P_D:

$$\gamma \equiv \Phi_L^V - \Phi_U^V, \quad P_D \equiv \Phi_L - \Phi_U, \quad P_D - \gamma \equiv \Phi_L^A - \Phi_U^A, \tag{9}$$

where $(\,)_L$ and $(\,)_U$ imply the upper and lower surface of the airfoil strip. It follows that

$$P_D = \gamma + \partial/\partial t \int_{-\infty}^{x} \gamma\,\mathrm{d}x. \tag{10}$$

For clarity of the development, the vorticity distribution on the airfoil ($-1 \leqslant x \leqslant +1$) is called γ_b, whereas the downstream vorticity in the wake ($x > 1$) is called γ_w. It is clear from the physics that $\gamma = 0$ for $y = 0$, upstream ($x < -1$). Thus, P_D can be written in terms of γ_w and Γ as follows:

$$x < -1: \quad P_D = \gamma = 0, \tag{11a}$$

$$-1 < x < +1: \quad P_D = \gamma_b + \partial/\partial t \int_{-1}^{x} \gamma_b\,\mathrm{d}x, \tag{11b}$$

$$x > 1: \quad P_D = 0 = \dot{\Gamma} + \gamma_w + \partial/\partial t \int_{+1}^{x} \gamma_w\,\mathrm{d}x, \tag{11c}$$

where Γ is the total bound circulation on the airfoil,

$$\Gamma \equiv \int_{-1}^{+1} \gamma_b \mathrm{d}x. \tag{12}$$

2.4. Vorticity transport and induced flow

From this follows immediately the vorticity transport relations

$$\begin{aligned}\frac{\partial P_D}{\partial x} &= \frac{\partial \gamma_b}{\partial x} + \frac{\partial \gamma_b}{\partial t}, \quad -1 < x < +1,\\ 0 &= \frac{\partial \gamma_w}{\partial x} + \frac{\partial \gamma_w}{\partial t}, \quad x > +1,\\ \gamma_w(x,t) &= -\frac{\partial \Gamma}{\partial t}(t - x + 1).\end{aligned} \tag{13}$$

where the last line is the solution to the ordinary differential equation in the second line with boundary condition from Eq. (11). Thus, the time rate of change of total bound circulation results in shed vorticity that enters the wake and is transported downstream at nondimensional velocity equal to unity.

The induced velocity from either bound or wake vorticity can be found from the Biot–Savart Law, applied to γ and broken up into γ_b and γ_w, namely.

$$v = -\frac{1}{2\pi}\int_{-1}^{\infty} \frac{\gamma}{x-\xi}\,\mathrm{d}\xi, \tag{14}$$

$$-v_b = +\frac{1}{2\pi}\int_{-1}^{+1} \frac{\gamma_b}{x-\xi}\,\mathrm{d}\xi \equiv v, \tag{15}$$

$$-v_w = +\frac{1}{2\pi}\int_{+1}^{\infty} \frac{\gamma_w}{x-\xi}\,\mathrm{d}\xi \equiv \lambda. \tag{16}$$

From the second line of Eq. (13) and the fact that, at every time step, a new piece of γ_w is shed into the wake, it follows that

$$\frac{\partial \lambda}{\partial t} + \frac{\partial \lambda}{\partial x} = \frac{1}{2\pi}\frac{\partial \Gamma/\partial t}{1-x}, \tag{17}$$

where v and λ are downwash due to bound and wake vorticity, respectively. Eqs. (1)–(17) complete the set of equations from potential flow theory that must be solved to form a thin-airfoil theory.

3. Thin airfoil theory as a feedback loop

3.1. Feedback loops

We are now in a position to view thin airfoil theory as a feedback system. Fig. 2 shows a block diagram that depicts the process. The input for thin airfoil theory is the nonpenetration boundary condition. Thus, the flow normal to the airfoil surface, w, must be countered by induced flow, ($w = v + \lambda$). It is assumed that the geometry, w, is specified. The induced flow due to bound vorticity ($v = w - \lambda$), once known, immediately gives the bound vorticity, γ_b through Eq. (15). Since this is not a differential equation, there is a straightforward linear, quasisteady mapping into γ_b. The bound circulation can then be fed back through Eq. (12) to obtain the total bound circulation (another quasisteady mapping); and Γ drives the differential equation, Eq. (17), to give the induced flow due to the wake, λ, which becomes the feedback mechanism. The closed-loop γ_b is taken through Eq. (11b) to give directly the desired air loads, P_D.

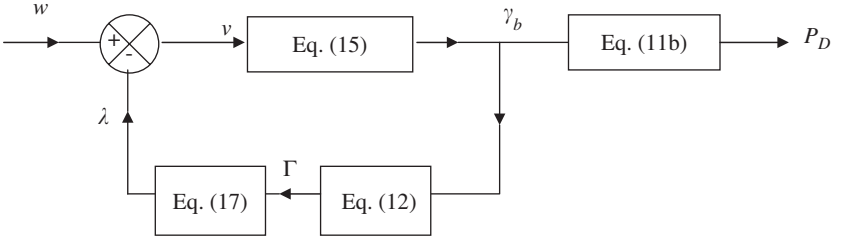

Fig. 2. Thin airfoil theory as a feedback loop.

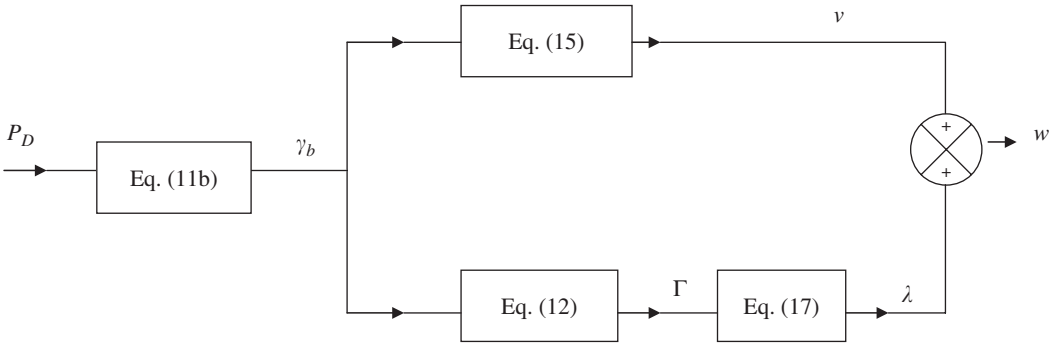

Fig. 3. Actuator strip theory.

Thin airfoil theory has historically concentrated on the solution to this closed-loop problem P_D/w. However, it is very useful to treat the forward and backward loops separately as two distinct theories. The backward loop is the induced-flow theory. That is, given the bound circulation (i.e., the strip loading) what is the induced flow due to the wake? The forward loop, Eq. (15), can be thought of as a lift theory. Given the distribution of angle of attack ($w-\lambda$), what will be the lift (i.e., bound circulation)? The Kutta condition comes into Eq. (11b) in that the system is only invertible if a constraint is placed on the loads, P_D. One of the side benefits of this type of formulation is that various stall models can be inserted in lieu of Eq. (15). Thus, this approach allows stall theories to be included without disturbing the inflow theory. The approach to be taken here is to develop a model that relates the bound vorticity (or, equivalently, the airfoil pressure distribution) to the induced flow due to the shed wake.

Fig. 3 shows a reconfiguration of the feedback loop in Fig. 2 that gives a typical actuator-strip theory, analogous to actuator disk theory for rotorcraft. The actuator strip theory gives a relationship for w/P_D (pressure in, velocity out). However, it is straightforward to see how v could be subtracted from w to obtain λ, if desired. Thus, one should also be able to obtain the Theodorsen function from merely the lower branch of Fig. 3 (as from the lower branch of the feedback loop of Fig. 2) with the appropriate closed-loop modification.

3.2. Glauert expansions

To turn the various partial differential equations into ordinary differential equations in time, it is necessary to expand the various airfoil quantities into Glauert expansions. These Glauert expansions are used in Classical Airfoil Theory (such as Theodorsen's) as well as in the finite-state vortex and potential models. The expansion functions are complete on the airfoil, and are derived from potential functions in elliptical coordinates. It is the elliptical coordinates that allow the discontinuity across the airfoil strip.

The transformation to elliptical coordinates is as follows:

$$x = \cos\varphi\,\cos\eta, \quad y = \sin\varphi\sin\eta. \tag{18}$$

Thus, for the upper airfoil surface, $\eta = 0$ and $0<\varphi<\pi$. The following are the basic expansions:

$$P_D = 2\left[\frac{\tau_s}{\sin\varphi} - \frac{\tau_a\cos\varphi}{\sin\varphi} + \sum_{n=1}^{\infty}\tau_n\sin(n\varphi)\right], \quad \gamma_b = 2\left[\frac{\gamma_s}{\sin\varphi} - \frac{\gamma_a\cos\varphi}{\sin\varphi} + \sum_{n=1}^{\infty}\gamma_n\sin(n\varphi)\right], \tag{19}$$

$$v = \sum_{n=0}^{\infty} v_n\cos(n\varphi), \quad \lambda = \sum_{n=0}^{\infty}\lambda_n\cos(n\varphi), \quad w = \sum_{n=0}^{\infty} w_n\cos(n\varphi). \tag{20}$$

With these expansions substituted into the operational equations, the partial differential equations and Biot–Savart integrals become ordinary differential equations and matrix transforms through the balancing of Glauert coefficients.

Thus, Eq. (11b) is transformed to

$$\begin{aligned}
&\gamma_s = \tau_s, \quad \gamma_a = \tau_a,\\
&\left(\dot\gamma_a - \frac{1}{2}\dot\gamma_2\right) + \gamma_1 = \tau_1 - \dot\Gamma/\pi,\\
&\frac{1}{2n}(\dot\gamma_{n-1} - \dot\gamma_{n+1}) + \gamma_n = \tau_n - \dot\Gamma/n\pi, \quad n = 2,3,4,\ldots.
\end{aligned} \tag{21}$$

which is a set of ordinary differential equations Eq. (12) becomes

$$\Gamma = 2\pi\left(\gamma_s + \frac{1}{2}\gamma_1\right) = 2\pi\left[(w_0 - \lambda_0) + \frac{1}{2}(w_1 - \lambda_1)\right] \tag{22}$$

and Eq. (15) becomes

$$v_0 = \gamma_a; \quad v_n = \gamma_n, \quad n = 1, 2, 3.... \tag{23}$$

Thus, these are simply constant transforms with no derivatives Eq. (17) becomes:

$$\dot{\lambda}_0 - \frac{1}{2}\dot{\lambda}_2 + \lambda_1 = \dot{\Gamma}/\pi, \quad \frac{1}{2n}(\dot{\lambda}_{n-1} - \dot{\lambda}_{n+1}) + \lambda_n = \dot{\Gamma}/n\pi, \quad n = 2, 3, 4 \ldots. \tag{24}$$

3.3. Pressure–velocity expressions

It is interesting that the sum of Eqs. (21) and (24) can be used to give an expression for w in terms of τ:

$$w_0 = \tau_a + \lambda_0, \quad \left(\dot{w}_0 - \frac{1}{2}\dot{w}_2\right) + w_1 = \tau_1, \quad \frac{1}{2n}(\dot{w}_{n-1} - \dot{w}_{n+1}) + w_n = \tau_n, \quad n = 2, 3, 4 \ldots \tag{25}$$

Thus, the only added information that is necessary to turn airfoil motion into airfoil loads is λ_0, the weighted average of inflow,

$$\lambda_0 = \frac{1}{\pi}\int_0^\pi \lambda \, \mathrm{d}\varphi, \quad \lambda_n = \frac{2}{\pi}\int_0^\pi \lambda \cos(n\varphi)\, \mathrm{d}\varphi. \tag{26}$$

From Eq. (24), one can see that λ_0 is coupled to the other λ_n and is driven by $\dot{\Gamma}$, the time rate of change of total bound circulation.

To satisfy the Kutta condition for a thin-airfoil theory, it is required that $\tau_s \equiv \tau_a$, which leads to $\gamma_s \equiv \gamma_a$. For an actuator-strip theory (making the analogy to a rotor) the Kutta condition is replaced by $\tau_s \equiv \tau_a = 0$, which gives no singularities in the pressure distribution. In fact, the pressure then becomes zero at the edges of the actuator strip. As stated earlier, either formulation can be used for the Theodorsen and Wagner functions.

4. Development of closed-form expressions

4.1. Lift expressions

The fluid dynamics and mathematics are now in place to develop closed-form expressions for the transfer functions in the Laplace domain, the transfer functions in the Fourier domain, and the step response in the time domain. To begin, we look at the most commonly used form, the frequency domain. In that formulation, the Theodorsen function is defined as the ratio of "circulatory lift" to "circulatory lift in the absence of the effect of wake-induced velocity." An important point here, however, is that the term "circulatory lift" has no absolute definition based on physics. One can see that all of the airloads (P_D) are due to bound vorticity γ_b. Thus, all lift is, strictly speaking, "circulatory." However, some authors define "circulatory lift" as the lift due to total bound circulation, which would be the quasistatic part of Eq. (11b) (Fung, 1995):

$$L_b = \Gamma = \int_{-1}^{+1} \gamma_b \, \mathrm{d}x = 2\pi\left(\gamma_s + \frac{1}{2}\gamma_1\right). \tag{27}$$

Under the Kutta condition, and with Eq. (24), this gives

$$L_b = \Gamma = 2\pi\left[\left(w_0 + \frac{1}{2}w_1\right) - \left(\lambda_0 + \frac{1}{2}\lambda_1\right)\right]. \tag{28}$$

For a rigid airfoil, $w_0 + \frac{1}{2}w_1$ is the angle of incidence at the three-quarter chord due to free stream. However, because the higher λ_n terms have a three-quarter chord contribution as well, $\lambda_0 + \frac{1}{2}\lambda_1$ is not precisely the angle of incidence at the three-quarter chord due to induced flow.

Not all authors, however, have defined "circulatory lift" in this way (Bisplinghoff et al., 1955). To understand why, it is instructive to write the unsteady lift in several forms from Eqs. (19), (21), (25) with the Kutta condition applied.

$$L/2\pi = \tau_a + \tfrac{1}{2}\tau_1, \tag{29a}$$

$$L/2\pi = \gamma_a + \tfrac{1}{2}\gamma_1 + \tfrac{1}{2}\dot{\gamma}_0 - \tfrac{1}{4}\dot{\gamma}_2 + \dot{\gamma}_s + \tfrac{1}{2}\dot{\gamma}_1 \doteq \hat{\Gamma} + \dot{\hat{\Gamma}} + \tfrac{1}{2}\dot{\gamma}_0 - \tfrac{1}{4}\dot{\gamma}_2, \tag{29b}$$

$$L/2\pi = (w_0 + \tfrac{1}{2}w_1) - (\lambda_0 + \tfrac{1}{2}\lambda_1) + \tfrac{3}{2}(\dot{w}_0 - \dot{\lambda}_0) + \tfrac{1}{2}(\dot{w}_1 - \dot{\lambda}_1) - \tfrac{1}{4}(\dot{w}_2 - \dot{\lambda}_2). \tag{29c}$$

Now, Eq. (29c) represents the quasi-steady and unsteady parts of the lift, with the first two terms being the lift due to total bound circulation, Eq. (22).

However, Eq. (24) can be used to write λ_n in terms of the other unsteady effects. The result in Eq. (29) is a cancellation of terms, which yields a simpler form of that equation,

$$L/2\pi = w_0 + \tfrac{1}{2}w_1 - \lambda_0 + \tfrac{1}{2}(\dot{w}_0 - \tfrac{1}{2}\dot{w}_2), \tag{30}$$

which can also be obtained directly from Eq. (25). Thus, Eq. (30) is an alternate form of the total lift. It is because of the simplicity of Eq. (30) as compared to Eq. (29) that most authors have elected to call $w_0 + \frac{1}{2}w_1 - \lambda_0$ the "circulatory lift", rather than the lift due to bound vorticity, $w_0 + \frac{1}{2}w_1 - \lambda_0 - \frac{1}{2}\lambda_1$. The unsteady term from Eq. (30), $\frac{1}{2}(\dot{w}_0 - \frac{1}{2}\dot{w}_2)$, is then called the apparent mass lift.

4.2. Circulatory lift

As stated above, most authors (Theodorsen, 1934) define the part of Eq. (30) without dots as the "circulatory lift", L_C:

$$L_C/2\pi \equiv w_0 + \tfrac{1}{2}w_1 - \lambda_0. \tag{31}$$

This is done for convenience and economy of derivation. Of course, this implies that L_C is not proportional to the bound circulation and that it is not approximated by the angle of incidence of the three-quarter chord.

Consequently, the Theodorsen function is defined as the ratio of $L_C/(L_C + \lambda_0)$. Thus, if all quantities are in the frequency domain, one can write

$$C(k) = \frac{w_0 + \frac{1}{2}w_1 - \lambda_0}{w_0 + \frac{1}{2}w_1} = \frac{\hat{\Gamma} + \frac{1}{2}\lambda_1}{\hat{\Gamma} + \lambda_0 + \frac{1}{2}\lambda_1}. \tag{32}$$

The same transfer function holds if these are in the Laplace domain. In that case, we call the function $D(s)$, which implies that $D(ik) = C(k)$. The Wagner function is defined as the response due to a step change in $(w_0 + \frac{1}{2}w_1)$, thus implying that the Wagner function is

$$w(t) = 1 - \lambda_0(t), \tag{33}$$

where λ_0 is the induced flow due to that step.

It is interesting to note how the transfer functions described above are closed-loop responses that can easily be formed from the open-loop responses $\lambda_0/\hat{\Gamma}$ and $\lambda_1/\hat{\Gamma}$. These open-loop responses represent the major transfer function in the feedback path of Fig. 2. It is easy to see from Eq. (32) that, once these open-loop responses are known (either in the time or frequency domain), $C(k)$ or $D(s)$ is immediately determined. The open-loop response of velocity due to bound vorticity is independent of boundary conditions or Kutta condition. It is simply the response of induced velocity to shed vorticity. Thus, the Theodorsen and Wagner functions are not, in themselves, dependent on the Kutta condition.

4.3. Derivation in frequency domain

Perhaps the most straightforward way to derive the Theodorsen function is to follow the approach of Sears (1940) and look at the induced flow due to a step input in $\hat{\Gamma}$. A step in $\hat{\Gamma}$ will give a single, concentrated vortex shed from the trailing edge of the airfoil at velocity of unity. The resultant induced flow distribution on the airfoil follows immediately from the Biot–Savart law:

$$\lambda(x,t) = \frac{1}{t+1-x}, \quad x > 1. \tag{34}$$

The important induced-flow components on the airfoil, λ_0 (uniform) and λ_1 (gradient), come immediately from the integrals in Eq. (26),

$$\lambda_0 = \frac{1}{\sqrt{t(2+t)}}, \quad \lambda_1 = \frac{2(t+1)}{\sqrt{t(2+t)}} - 1. \tag{35}$$

The combinations formed in the Theodorsen function are

$$1+\tfrac{1}{2}\lambda_1=\frac{t+1}{\sqrt{t(2+t)}},\quad 1+\lambda_0+\tfrac{1}{2}\lambda_1=\sqrt{\frac{2+t}{t}}. \tag{36}$$

It is perhaps easiest now to move to the Laplace domain. We take the Laplace transform of the step response,

$$\mathscr{L}[\lambda_0]=e^s K_0(s),\quad \mathscr{L}\left[1+\tfrac{1}{2}\lambda_1\right]=e^s K_1(s). \tag{37}$$

This, multiplied by s, gives the impulse response. Immediately, we have the complex version of the Theodorsen function from Eq. (32):

$$D(s)=\frac{e^s K_1(s)}{e^s K_0(s)+e^s K_1(s)}=\frac{K_1(s)}{K_0(s)+K_1(s)}, \tag{38}$$

where we have used the fact that the transfer function is the Laplace transform of the impulse response, which is the Laplace transform of the step response multiplied by s. The Theodorsen function follows immediately as

$$C(k)=\frac{K_1(ik)}{K_0(ik)+K_1(ik)}\equiv\frac{J_1-iY_1}{J_1-iY_1+i(J_0-iY_0)}. \tag{39}$$

4.4. Time domain

Next, we come to the step response of lift due to $w_0+\frac{1}{2}w_1$, which gives us the Wagner function. Once again, we use the fact that the step response is the impulse response divided by s. Thus, we have

$$W(t)=\frac{1}{2\pi i}\int_{c-i\infty}^{c+i\infty}\frac{D(s)}{s}e^{st}ds, \tag{40}$$

where $D(s)$ is given by Eq. (38). Eq. (40) is, in itself, the correct form of the Wagner function, $W(t)$. On the other hand, it is usually more convenient to put it into Fourier transform form. A problem with this, however, is that the integrand of Eq. (40) has a pole on the imaginary axis at $s=0$. This is because

$$D(0)=1,\quad D(ik)=C(k),\quad C(0)=1,\quad C(\infty)=\tfrac{1}{2}. \tag{41}$$

Thus, $D(s)/s$ is infinite at $s=0$. Therefore, before changing to a Fourier transform, the pole must be removed:

$$W(t)=\frac{1}{2\pi i}\int_{c-i\infty}^{c+i\infty}\left[\frac{D(s)-D(0)}{s}e^{st}+\frac{D(0)}{s}e^{st}\right]ds=D(0)\bar{u}(t)+\frac{1}{2\pi i}\int_{c-i\infty}^{c+i\infty}\left[\frac{D(s)-D(0)}{s}e^{st}\right]e^{st}\,ds. \tag{42}$$

Now, the second term in the second line can accommodate $c\equiv 0$, converting it to a Fourier transform with $s=ik$.

$$W(t)=\bar{u}(t)+\frac{1}{2\pi i}\int_{-\infty}^{+\infty}\frac{C(k)-1}{k}e^{ikt}\,dk=\bar{u}(t)+\frac{1}{\pi}\int_0^\infty\left[\frac{\mathrm{Re}C(k)-1}{k}\right]\sin kt\,dk$$
$$+\frac{1}{\pi}\int_0^\infty\frac{\mathrm{Im}C(k)}{k}\cos kt\,dk. \tag{43}$$

The fact that $W(t)\equiv 0$ for negative t further implies that the two integrals in the second part of Eq. (43) must be equal. Since $\int_0^\infty[(\sin kt/k]\,dk=\pi/2$ and since $W(t)\equiv 0$ for negative t, we can rewrite $W(t)$ in several ways. Thus we have for $t>0$,

$$W(t)=1+\frac{2}{\pi}\int_0^\infty\left[\frac{\mathrm{Re}C(k)-1}{k}\right]\sin(kt)\,dk \tag{44a}$$

$$=\frac{2}{\pi}\int_0^\infty\frac{\mathrm{Re}C(k)}{k}\sin(kt)\,dk \tag{44b}$$

$$=\frac{1}{2}+\frac{2}{\pi}\int_0^\infty\left[\frac{\mathrm{Re}C(k)-\frac{1}{2}}{k}\right]\sin(kt)\,dk \tag{44c}$$

$$=1+\frac{2}{\pi}\int_0^\infty\frac{\mathrm{Im}C(k)}{k}\cos(kt)\,dk. \tag{44d}$$

For numerical work, Eq. (44a) is usually the best behaved, although Eq. (44c) is useful for small t, and Eq. (44d) is useful for large t. The second line, Eq. (44b), although the most compact, is not numerically well conditioned.

Interestingly, the above development proves that $W(0)=\frac{1}{2}$ based on Eq. (44c). In particular, this is true because $C(k)\to\frac{1}{2}$ as $k\to\infty$, and the integral limit as $t\to 0$ has no contribution even under the infinite domain for which k is integrated. In a similar manner, either line of Eq. (44) can be used to show that $W(\infty)=0$.

5. Finite-state models

5.1. Basis

Many finite-state models of unsteady aerodynamics are based on a fit of either the Theodorsen function (in the frequency domain) or of the Wagner function (in the time domain). Here we consider finite-state models from first principles based on the fluid dynamic equations shown earlier in this paper. In one sense, there can be no formal closed-form finite-state model since the Bessel functions $K_0(s)$ and $K_1(s)$ yield no poles in the domain, but a branch cut. However, a branch cut can be approximated by a distribution of poles. Thus, an approximate finite-state model is possible. On the other hand, since the location of the branch cut is rather arbitrary in the s-domain, it follows that there will be no single, unique finite-state model; and each possible model will have different convergence properties.

The lack of a true finite-state model can be seen from two aspects of the Theodorsen function $C(k)$ at small k. In particular, at small k the $\mathrm{Re}[C(k)]$ is approximated by $1-\pi k/2$. Thus $d\,\mathrm{Re}[C]/\mathrm{d}k\neq 0$ at $k=0$. Now, any finite-state model will, necessarily, have $d\,\mathrm{Re}[C]/\mathrm{d}k\equiv 0$ at $k=0$. Thus, there is always a "boundary layer" in k for which the behavior of $\mathrm{Re}[C(k)]$ is not properly modeled. However, as will be seen in the results to follow, this boundary layer decreases in width as the number of states is increased.

A similar phenomenon occurs in the $\mathrm{Im}[C(k)]$ which behaves as $-k\ln(k)$ for small k. Thus $d[\mathrm{Im}C]/\mathrm{d}k=-\infty$ at $k=0$. No finite-state model can have an infinite slope of the imaginary part of the transfer function. However, as more states are added, this slope will become larger and larger in the model. A similar trend can be seen in the Wagner function. There, as seen in Eq. (34), the decay of $W(t)$ for large t must be of the form $1/t$. However, finite-state models will always decay as $e^{-\beta t}$, never as $1/t$. Once again though, as more states are added, the finite-state model will approximate $1/t$ to greater and greater accuracy.

5.2. Vortex-based models

This brings us to the first class of finite-state models, the vortex-based approach (Peters and Karunamoorthy, 1993, 1994). This approach takes the ordinary differential equations developed earlier in this report and applies them directly with the λ_n as the states. The states of the model are, therefore, the inflow distributions due to shed vorticity. The appropriate equations include either Eqs. (24) and (25) or (equivalently) Eqs. (24) and (21), although the former is preferred. One interesting aspect of this, however, is that this set of equations is not quite complete. One can notice from Eq. (24) that there is no equation with a static λ_0 term. Thus, one more equation is needed to complete the set.

In Peters and Karunamoorthy (1993, 1994), it is shown that the extra equation can be obtained based on Eqs. (14) and (26). In particular, the extra equation is based on the observation of Sears (1940) that, for finite time, the wake does not go to infinity. It only extends to $x=t$. This means that $x=\infty$ can be excluded from the domain. To show how this allows another equation, let $X\equiv e^{-\eta}$ in elliptical coordinates. It is shown in Johnson (1980) that λ_n can be written as an integral from 0 to infinity that involves X^n. However, the integral for λ_0 is undefined because X^0 does not decay. On the other hand, if we note that the wake does not extend to infinity, we can approximate X^0 by a series in X^n over $0<X\leqslant 1(\infty<\eta\leqslant 0)$. At the trailing edge ($x=1$, $\eta=0$), we have $X=1$. In the far wake ($x\to\infty$, $\eta\to\infty$), we have $X=0$. Thus, if one can fit 1 by a polynomial in X^n ($0<X\leqslant 1$), then one can express λ_0 in terms of the λ_n for finite time (Peters and Karunamoorthy, 1993, 1994). Thus, if

$$1\approx\sum_{n=1}^{N}b_nX^n,\quad 0<X\leqslant 1, \tag{45}$$

then

$$\lambda_0\approx\frac{1}{2}\sum_{n=1}^{N}b_n\lambda_n. \tag{46}$$

Eq. (46) thus becomes the extra equation that completes the set of Eq. (24).

There are an infinite number of ways to choose the b_n based on how the fit is to be weighted. (Obviously, the point $X=0$ is always weighted to be zero.) It turns out that, if the fit in Eq. (45) is constrained to be exact at $X=1$, then $\sum_{n=1}^{N} b_n = 1$. Peters et al. (1995) point out that this ensures that $C(k)$ will approach $\frac{1}{2}$ at $k\to\infty$ as the number of states is increased. If, in addition, $\sum_{n=1}^{N} n b_n = 0$ (implying that the slope of the fit is constrained to be zero at $X=1$, the trailing edge), then $C(k)\equiv 0.5$ at $k=\infty$ even for the finite-state model with truncated states.

Peters et al. (1995) offer two possible approximations for b_n. One is the binomial approximation

$$b_n = (-1)^{n-1}\frac{N!}{n!(N-n)!}. \tag{47}$$

This weights the near-airfoil more than it does the downstream and, thus, is more accurate at smaller reduced time. It satisfies $\sum b_n = 1$ and $\sum n b_n = 0$. Another approach is a least-squares fit, and this gives a more uniform approximation for large time.

$$\begin{aligned} b_n &= (-1)^{n-1}\frac{(N+n-1)!}{(N-n-1)!}\frac{1}{(n!)^2}, \quad 1<n<N-1,\\ b_N &= (-1)^{N+1}. \end{aligned} \tag{48}$$

Eq. (24), augmented with Eq. (46) then becomes a vorticity-based, finite-state model. The $b_N = (-1)^{n+1}$ ensures $\sum b_n = 1$.

5.3. Galerkin-based models

A second approach to finite-state thin airfoil theory is to apply Galerkin's method directly to the potential flow equations, Eq. (2) (Peters and Nelson, 2000a, b; Nelson, 2001). This involves expansion of the velocity potential Φ^V, Eq. (5), in terms of potential functions Ψ^α and Ψ^β. We begin with the solutions to the Laplace's equation in elliptical coordinates, as given below,

$$\begin{aligned} &f_n \equiv \frac{1}{n}e^{-n\eta}\sin(n\varphi), \quad g_n \equiv \frac{1}{n}e^{-n\eta}\cos(n\varphi),\\ &f_0 = \varphi, \quad g_0 = \eta - K. \end{aligned} \tag{49}$$

where $K=\eta_{\max}$, the maximum η for which the wake is considered.

The velocity potentials are then expressed in terms of Ψ_n^α and Ψ_n^β where

$$\Psi_n^\alpha = \frac{1}{2}(-g_{n+1}+g_{n-1}), \quad \Psi_n^\beta = \frac{1}{2}(f_{n+1}-f_{n-1}). \tag{50}$$

These are placed into the momentum equation and dotted with the gradient of the test functions (f_0 and g_0, $n=0$) and (nf_n and ng_n, $n=1,\ldots,n$). The equations are then integrated over the upper-half plane ($0<\varphi<\pi$ and $0<\eta<\mathrm{K}$) with use of the Divergence Theorem to obtain the equations in a typical Galerkin fashion.

Interestingly, for two elements of the matrix, the integral out to $\mathrm{K}=\eta_{\max}$ will approach infinity as $\mathrm{K}\to\infty$. Rather than choosing some arbitrary K to limit these integrals, Nelson (2001) chooses the same b_n expansion for unity as is used in the vortex methods to limit these values. Thus, the integral of X^{-1} gives $\ln|X| = -\eta$ which gives for b_n from Eq. (47):

$$\mathrm{K} = \lim_{\eta\to\infty}\frac{\pi}{2}\eta = \frac{\pi}{2}\sum_{n=1}^{N}\frac{b_n}{n} = \frac{\pi}{2}\sum_{n=1}^{N}\frac{1}{n}. \tag{51}$$

It can be demonstrated that, as $N\to\infty$, this sum will approach infinity, as it ought. Thus, K is replaced by Eq. (51) in the infinite integrals.

The final form of the equation is as follows:

$$\begin{aligned} &\Psi = \sum_{n=1}^{N}\left[\alpha_n\psi_n^\alpha + \beta_n\Psi_n^\beta\right],\\ &u = \partial\Psi/\partial x, \quad v = -\partial\Psi/\partial y, \end{aligned} \tag{52}$$

$$\begin{bmatrix} M & Q^{\mathrm{T}}\\ Q & M\end{bmatrix}\begin{Bmatrix}\dot\alpha\\ \dot\beta\end{Bmatrix} + \begin{bmatrix} S^{\mathrm{T}} & -d\\ d & S^{\mathrm{T}}\end{bmatrix}\begin{Bmatrix}\alpha\\ \beta\end{Bmatrix} = \begin{bmatrix} d & S^{\mathrm{T}}\\ S & d\end{bmatrix}\begin{Bmatrix}\tau\\ 0\end{Bmatrix}, \tag{53}$$

where the row subscripts are $l = 0,1,2,3,\ldots$, and the column subscripts are $n = 1,2,3,4,\ldots$. The τ_n are the pressure expansion terms, Eq. (19).

The matrix elements become ($l \neq 0$) as below:

$$\begin{gathered} M_{ln} = \frac{4ln}{4l^2n^2 - (l^2+n^2-1)^2}, \quad l+n \text{ even}; \quad M_{ln} = 0, \quad l+n \text{ odd}; \\ Q_{ln} = +\frac{\pi}{4}, \quad n = l+1; \quad Q_{ln} = -\frac{\pi}{4}, \quad n = l-1; \quad Q_{ln} = 0, \quad n \neq l \pm 1; \\ S_{ln} = \frac{2ln}{(n^2-l^2)}, \quad l+n \text{ odd}; \quad S_{ln} = 0, \quad l+n \text{ even}; \\ d_{ln} = \frac{l\pi}{2}, \quad l = n; \quad d_{ln} = 0 \quad l \neq n. \end{gathered} \tag{54}$$

The following changes to Eq. (54) must be made for the case $l = 0$. First, M_{ln} and S_{ln} must be divided by l and then l set equal to zero. Second, $Q_{01} = -Q_{10} = \frac{\pi}{2}\sum_{n=1}^{N} 1/n$, which approaches infinity as the number of states increases. Third, $M_{01} = \pi^2/4$ rather than the zero that Eq. (54) would imply for $l+n$ odd. The proof of these values is given in Nelson (2001). With this, Eqs. (52) and (53) become a Galerkin-based finite-state model.

5.4. Applications

An interesting aspect of the finite-state models is their diversity of applications. Because they are in the form of ordinary differential equations, they can be used in many modes. For example, the Laplace transform can be utilized to obtain an approximation for $D(s)$; or, $s = ik$ can be used to obtain the transfer function in the frequency domain. The equations can be time-marched, or one can obtain an eigenvalue solution. Most importantly, the airloads equations can be assembled into a larger, structural dynamic framework in which one can do either eigenvalue analysis or any other types of analysis. Peters and Johnson (1994) and Peters et al. (1995) show how this formulation is easily coupled with an unsteady free-stream or dynamic stall model in both fixed-wing and rotary-wing applications.

Finite difference models are also state-space models since the assembly of the difference equations gives a set of states equal to the number of computational nodes. However, as compared to finite-state models, finite difference equations result in a very large number of states. Further, the incompressibility condition is an unwieldy constraint that makes the solution process very difficult. Thus, artificial compressibility is often introduced into finite difference solutions for incompressible potential flow. Dowell (1996) discusses other ways to reduce the order of finite-difference models.

6. Results

6.1. Vortex-based model

It is informative to compare calculations from the finite-state models to closed-form results. Fig. 4 shows both the Real and Imaginary parts of $C(k)$ as well as the Wagner step function $W(t)$ for the vortex-based finite-state model with only four states. The exact Theodorsen and Wagner functions are also plotted (XCT). The exact Wagner function is based on the integral in Eq. (44a). Two versions of the finite-state model are shown, one with the binomial expansion (BNX) and one with the least-squares fit with constraint (AUG). Results are plotted versus $k/(1+k)$ and $\tau/(1+\tau)$ in order to show the entire frequency and time scale range on a scale from zero to unity. (Note that $\tau \equiv t$.) One can see several points mentioned earlier in the paper. First, all finite-state results have zero slope at $k = 0$ for $\mathrm{Re}C(k)$ and they have a finite slope for $\mathrm{Im}\, C(k)$. The binomial weighting does better than augmented at low t (large k), but the least squares does better overall. Fig. 5 shows the same results for eight states. One can see how both weighting methods are now much closer to the exact solution, which corroborates the convergence to the exact solution. Table 1 shows error two-norms over both the entire frequency and the entire time domain for $|C(k)|$ and $|W|$, respectively, where the integrals are taken over $k/(1+k)$ and $\tau/(1+\tau)$. The classical Jones result and some Padé approximants are also analyzed for this same norm. For the Padé approximants, a Bode plot is fit to $C(k)$ to give the best fit. One can see a uniform convergence of the vortex-based method up until a point where ill conditioning implies greater numerical precision is needed. This shows that the main obstacle to convergence of the finite-state model is the ill-conditioned nature of the matrices as N becomes large. This is due to the nature of approximating a branch cut by poles. Nevertheless, the convergence of all finite-state results with $N = 8$ is good.

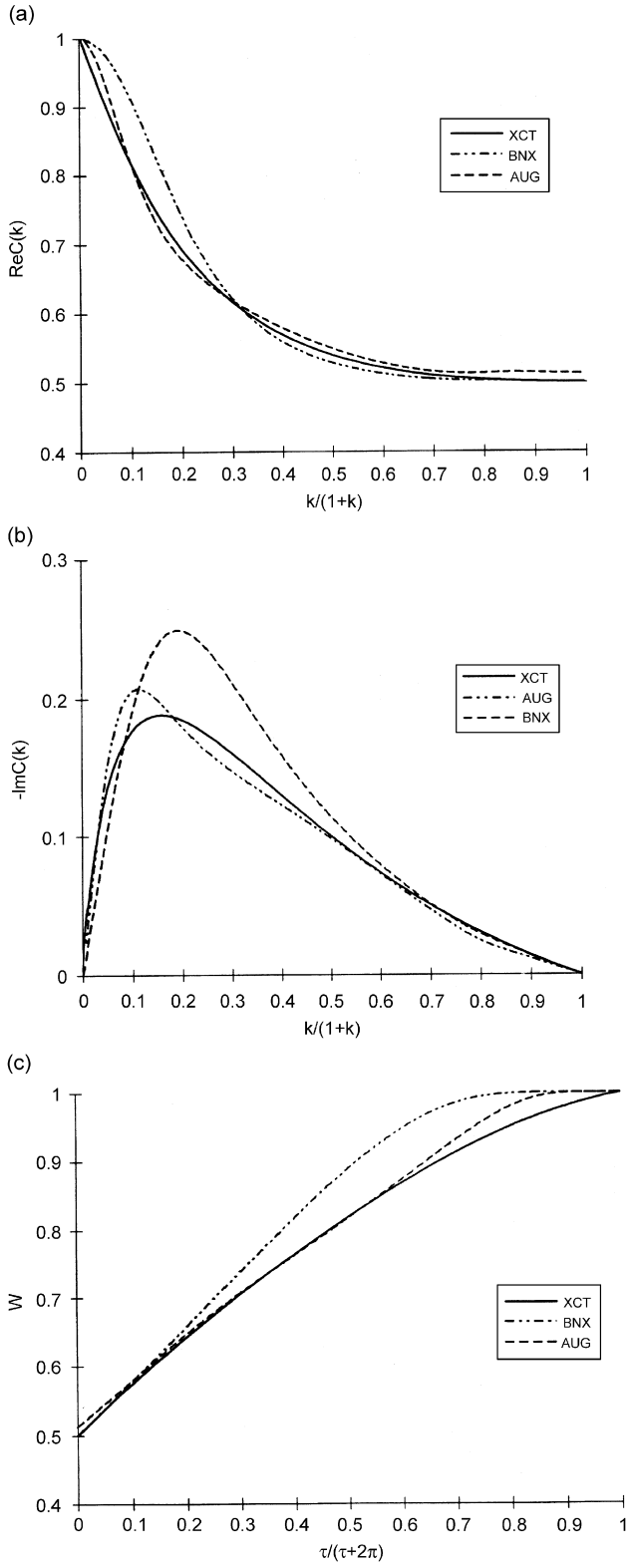

Fig. 4. (a) Real part of $C(k)$, 4 states; (b) imaginary part of $C(k)$, 4 states; (c) Wagner function, $W(t)$, 4 states.

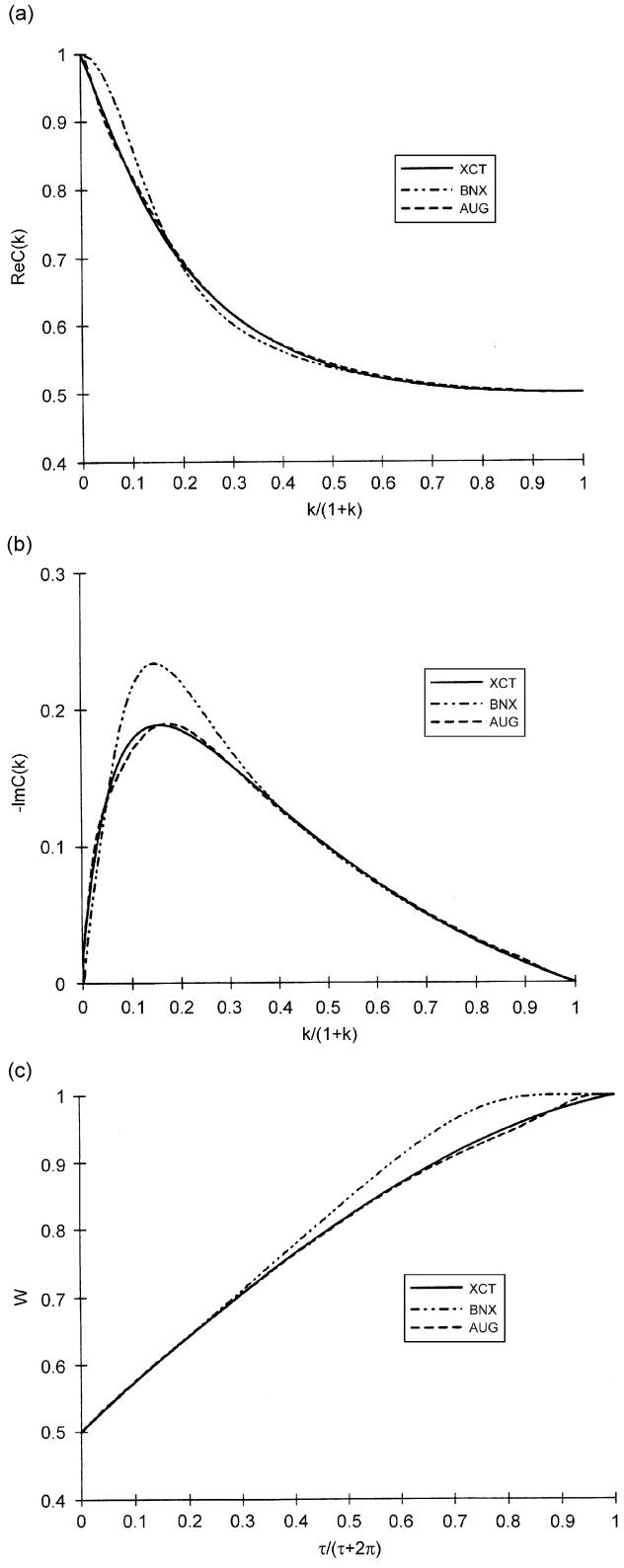

Fig. 5. (a) Real part of $C(k)$, 8 states; (b) imaginary part of $C(k)$, 8 states; (c) Wagner function, $W(t)$, 8 states.

6.2. Galerkin-based model

Next, we turn to the convergence of the Galerkin-based model of Nelson (2001). For comparison purposes, we treat the airfoil as an actuator-strip and do not apply the Kutta condition. Rather, we apply a given pressure distribution τ_n at a desired reduced frequency k. The normal component of induced flow along the y-axis is given in Figs. 6–8, which are for $k = 0$, 1 and 4, respectively. Both real (in-phase) and imaginary (out-of-phase) responses are shown. Also shown on the plot are: (i) the "Exact" solution (which is obtained by a convolution integral) and (ii) a vortex-based result, labeled "Ref. [18]." The vortex-based result only gives the flow on the disk (not off the disk). The Galerkin results have 28 states and the vortex-based results have eight states with the augmented b_n.

Both Galerkin and vortex-based methods do quite well on the disk. The reason that the Galerkin-based approach requires more states than the vortex model is that it yields more information than does the vortex method. The latter gives only normal velocity for $-1 < x < +1$, whereas the Galerkin gives all three components of velocity everywhere in the upper half plane. The results in Figs. 6–8 as well as the more detailed results in Nelson (2001) show that the Galerkin method converges slowly for the inflow in the wake ($x > 1$) because that inflow does not decay as $x \to \infty$.

Although the above results do not include the Kutta condition, they are still quite applicable to computation of the Theodorsen function. Fig. 9 gives the same error norm as defined in Table 1 for $C(k)$ as computed by the Galerkin method with 28 states. Up to a reduced frequency of about 3.0, the average error norm is about 5%, which is comparable to the error of vortex models with four to eight states. This is because the Galerkin approach optimizes the error of the entire flow field while the vortex-model concentrates only on one component of on-disk flow. For $k \geqslant 4.0$, the cost of trying to converge on the flow in the wake implies that errors of 15–30% occur on the average flow on the airfoil. (This flow diminishes as k increases.) In other words, the mean flow λ_0 (which dominates $C(k)$) is decreasing with k as the oscillatory flow in the wake increases with k, making $C(k)$ less accurate in a Galerkin approach. However, as Figs. 6–8 show, the total flow on the airfoil remains well approximated by the Galerkin method even at $k = 4.0$.

It is the nature of finite-state methods that they can be designed for certain applications. Binomial weighting is optimum for short time (large k), whereas the augmented method is better at large time (small k). The Galerkin method is optimized for the total velocity field whereas vortex models are optimized for on-airfoil flow.

7. Summary and conclusions

Two-dimensional, incompressible unsteady airfoil theory is based on a set of fairly compact equations for conservation of mass and momentum (i.e., the potential flow equations) that can be transformed into vorticity equations. Glauert expansions of the terms in these equations are very useful in both the solution and the interpretation of thin airfoil theory. With these expansions in hand, a simple step response for the velocity field due to a single, trailed vortex leads immediately to the Laplace-form and frequency-form of the lift deficiency function (i.e., the Theodorsen

Table 1
Error norms

Methods	Theodorsen (%)	Wagner (%)
Curve-fit		
Jones	2.3	1.8
Padé, $N = 2$	2.1	3.8
Padé, $N = 3$	1.2	3.4
Augmented		
$N = 4$	3.5	5.0
$N = 6$	1.6	1.8
$N = 8$	1.0	1.3
Binomial		
$N = 4$	10.5	18.3
$N = 8$	5.6	10.1
$N = 16$	2.8	5.0
$N = 30$	1.3	–
$N = 50$	0.7	–

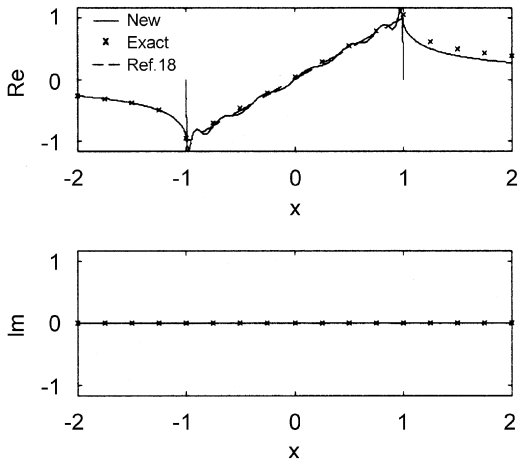

Fig. 6. Inflow at $k = 0$.

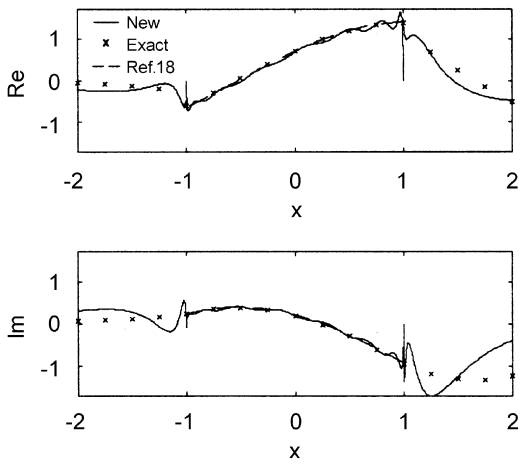

Fig. 7. Inflow at $k = 1$.

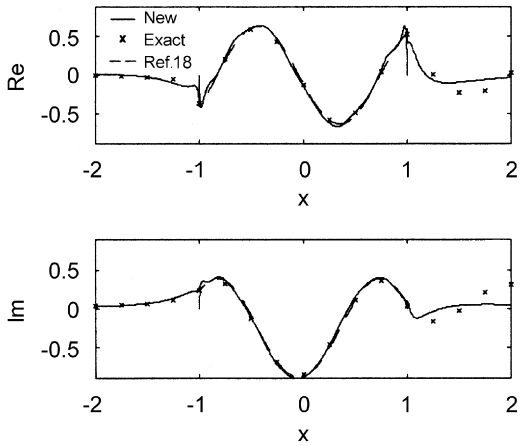

Fig. 8. Inflow at $k = 4$.

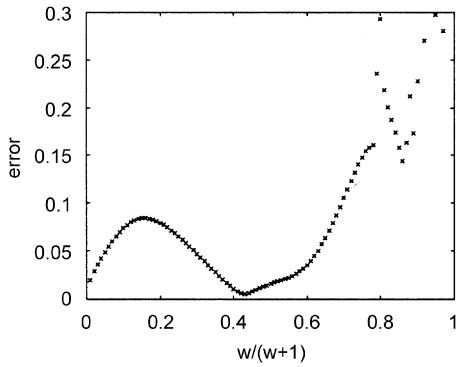

Fig. 9. Error norm between the Theodorsen function and the new formulation.

function) and to the step response of an airfoil, the Wagner function. These forms are related to each other through their Fourier transforms.

The same Glauert expansions can also yield finite-state inflow models, in which the induced flow is represented in terms of a finite number of states that measure the strength of closed-form potential functions. Models can be developed

either from the vorticity equations or from the potential flow equations. Because of the singular nature of the two-dimensional problem, there are singularities that arise in both derivations; but these can be treated by noting that the wake does not trail to infinity. As a result, the infinity can be approximated yielding convergent inflow models by either approach.

Numerical results have shown that the finite-state results give good correlation with the more conventional, frequency-domain versions. The advantages of the finite-state methodology, however, are clear:

(i) the inflow theory can be coupled with lift models other than the simple non-penetration boundary condition of classical theories;
(ii) finite-state models are in a matrix form that allows them to be easily assembled together with structural models for aeroelastic computations;
(iii) the finite-state models permit solutions in either the time domain, the frequency domain, or the Laplace domain for arbitrary forcing functions and even for unsteady free-stream.

Thus, they can be applied to a much wider variety of problems than can classical approaches.

Acknowledgment

The work in this paper was sponsored through the National Rotorcraft Technology Center through the Georgia Tech/ Washington University Center of Excellence for Rotorcraft Technology.

Appendix A. Non-dimensional quantities

In the foregoing derivation, all velocities are made nondimensional on the free-stream velocity, all lengths are made nondimensional on the semi-chord, and (it follows that) time is made nondimensional on the semi-chord divided by free-stream velocity. All pressures are made nondimensional on the density of the fluid times the free-stream squared. It follows that lift per unit span is made nondimensional on ρbU^2 and pitching moment on ρb^2U^2.

Appendix B. Pitching moment

Although the above development focuses on the airfoil lift per unit length, the pitching moment follows directly. The nondimensional pitching moment per unit length about mid-span, M_0, is given by

$$\frac{M_0}{2\pi} = -\frac{\tau_a}{2} + \frac{\tau_2}{4}. \tag{55}$$

It follows that the nose-up pitching moment about the quarter-chord is given by

$$\frac{M_{3/4}}{2\pi} = \frac{1}{4}(w_1 + w_2) + \frac{1}{4}\dot{w}_0 + \frac{1}{16}\dot{w}_1 - \frac{1}{8}\dot{w}_2 - \frac{1}{16}\dot{w}_3. \tag{56}$$

This gives the Theodorsen moment. Interestingly, the moment about the quarter-chord is independent of λ_0 (as well as being independent of all λ_n) and thus it is independent of the Theodorsen function.

References

Beddoes, T.S., 1983. Representation of airfoil behavior. Vertica 7, 183–197.

Bisplinghoff, R.L., Ashley, H., Halfman, R.L., 1955. Aeroelasticity. Addison-Wesley, Reading, MA.

Dinyavari, M.A.H., Friedmann, P.P., 1984. Unsteady aerodynamics in time and frequency domains for finite time arbitrary motion of rotary wings in hover and forward flight. AIAA Paper 84–0988.

Dowell, E.H., 1980. A simple method for converting frequency domain aerodynamics to the time domain. NASA TM-81844.

Dowell, EarlH., 1996. Eigenmode analysis in unsteady aerodynamics: reduced-order models. AIAA Journal 34, 1578–1583.

Edwards, J.W., Breakwell, J.V., Bryson Jr., A.E., 1978. Active flutter control using generalized unsteady aerodynamic theory. Journal of Guidance and Control 1, 32–40.

Edwards, J.W., Ashley, H., Breakwell, J.V., 1979. Unsteady aerodynamic modeling for arbitrary motions. AIAA Journal 17, 365–374.

Edwards, J.W., Breakwell, J.V., Bryson Jr., A.E., 1989. Reply by authors to Vepa. Journal of Guidance and Control 2, 447–448.
Fung, Y.C., 1995. An Introduction to the Theory of Aerolesticity. Wiley, New York.
Garrick, I.E., 1938. On some reciprocal relations in the theory of nonstationary flows. NACA Report 629.
Hassig, H.J., 1971. An approximate true damping solution of the flutter equations by determinant iteration. Journal of Aircraft 8, 825–889.
Johnson, W., 1980. Helicopter Theory. Princeton University Press, 477pp.
Jones, R.T., 1938. Operational treatment of the nonuniform lift theory to airplane dynamics. NACA TN 667, 347–350.
Jones, R.T., 1939. The unsteady lift of a wing of finite aspect ratio. NACA Report 681, 31–38.
Jones, W.P., 1945. Aerodynamic forces on wings in non-uniform motion. British Aeronautical Research Council, R & M 2117.
Loewy, R.G., 1957. A two-dimensional approximation to unsteady aerodynamics in rotary wings. Journal of the Aeronautical Sciences 24, 81–92.
Nelson, A.M., 2001. Inflow equations in two dimensions from a Galerkin approach. Master of Science Thesis, Washington University in St. Louis.
Peters, D.A., Karunamoorthy, S., Cao, W., 1995. Finite-state induced flow models, Part I: two-dimensional thin airfoil. Journal of Aircraft 44, 1–28.
Peters, D.A., Barwey, D. and Johnson, M.J., 1995. Finite-state airloads modeling with compressibility and unsteady free-stream. In: Sixth International Workshop on Dynamics and Aeroelastic Stability Modelling of Rotorcraft systems, UCLA.
Peters, D.A., Johnson, M.J., 1994. Finite-state airloads for deformable airfoils on fixed and rotating wings. Aeroelasticity and Fluid/Structures Interaction Problems, a Mini-Symposium. ASME Winter Annual Meeting, Chicago, 44, pp. 1–28.
Peters, D.A., Karunamoorthy, S., 1993, 1994. State-space inflow models for rotor aeroelasticity. In: Proceedings of the Holt Ashley 70th Anniversary Symposium, Stanford University, 1993 and AIAA 12th Applied Aerodynamics Conference, Colorado Springs, USA.
Peters, D.A., Nelson, A.M., 2000a. A two-dimensional rotor inflow model developed in closed form from a Galerkin approach. In: Proceedings of the 18th AIAA Applied Aerodynamics Conference, Paper AIAA-2000-4119.
Peters, D.A., Nelson, A.M., 2000b. A Dynamic Wake Model in Two Dimensions from a Galerkin Approach. AHS Aeromechanics Specialists' Meeting, Atlanta, Georgia, USA.
Sears, W.R., 1940. Operational methods in the theory of airfoils in non-uniform motion. Journal of the Franklin Institute 230, 95–111.
Theodorsen, T., 1934. General theory of aerodynamic instability and the mechanism of flutter. NACA Report 496, 413–433.
Vepa, R., 1976. On the use of Padé approximants to represent unsteady aerodynamic loads for arbitrarily small motions of wings. AIAA Paper, pp. 7–17.
Wagner, H., 1925. Uber die entstehung des dynamischen auftriebs von tragflugeln. ZAMM 5, 17–35.